Observation of CH A→X, CN B→X, and NH A→X emissions in gasphase collisions of fast O(3 P) atoms with hydrazines

Otto J. Orient, Ara Chutjian, and Edmond Murad

Citation: The Journal of Chemical Physics **101**, 8297 (1994); doi: 10.1063/1.468095
View online: http://dx.doi.org/10.1063/1.468095
View Table of Contents: http://scitation.aip.org/content/aip/journal/jcp/101/10?ver=pdfcov
Published by the AIP Publishing

Observation of CH $A \rightarrow X$, CN $B \rightarrow X$, and NH $A \rightarrow X$ emissions in gas-phase collisions of fast O(^3P) atoms with hydrazines

Otto J. Orient and Ara Chutjian
Jet Propulsion Laboratory, California Institute of Technology, Pasadena, California 91109

Edmond Murad
Phillips Laboratory/WSCI, 29 Randolph Road, Hanscom AFB, Massachusetts 01731-3010

(Received 1 June 1994; accepted 1 August 1994)

Optical emissions in single-collision reactions of fast (20 eV laboratory translational energy) O(^3P) atoms with hydrazine, methylhydrazine, and 1,1-dimethylhydrazine have been measured in a crossed-beams geometry. The emissions were observed in the wavelength range 325–440 nm, and were identified as the CH ($A\ ^2\Delta \rightarrow X\ ^2\Pi_r$) (for methylhydrazine), CN ($B\ ^2\Sigma^+ \rightarrow X\ ^2\Sigma^+$) (for methylhydrazine), and NH ($A\ ^3\Pi \rightarrow X\ ^3\Sigma^-$) transitions (for all three hydrazines). The experimental vibration-rotation bands were fit to a synthetic spectrum of CH, CN, and NH with given vibrational and rotational temperatures.

I. INTRODUCTION

Collision studies of hyperthermal neutral beams with molecules under single-collision (nonplasma) conditions provide evidence for considerable chemical reaction and bond disruption in the collision system.[1–3] Such studies also provide a means of selectively pumping a single (translational) degree of freedom and probing its effects on chemical reactivity. For the case of endothermic processes, measurements of the reaction *threshold* can provide information on the barrier for the reaction, and how that barrier is related to reaction dynamics (e.g., on the symmetry of the colliding partners).[4,5] In a previous study of the reaction O(^3P)+HCN it was shown that the measured threshold for the CN ($B \rightarrow X$) transition was in good agreement with the thermochemical threshold, indicating a small reaction barrier.[3]

Reported herein is a study of the reaction of fast [laboratory (LAB) energies of 20 eV] O(^3P) atoms with a sequence of three increasingly complex molecules, N_2H_4, $CH_3NH–NH_2$, and 1,1-$(CH_3)_2N–NH_2$ under single-collision, beam–beam conditions. The study was undertaken to identify the reaction channel(s) which are active in the hyperthermal energy regime, to compare observations with data from thermal-energy studies, and to apply the results of the laboratory work to experimental data from low-earth orbit (LEO) space experiments.

In this last regard, CN ($B \rightarrow X$) was observed when the shuttle primary reaction control engines were fired into the ambient atmosphere.[6] The velocity of the exhaust gases was the sum of the LEO velocity (7.8 km/s) and the exhaust-gas velocity (3.5 km/s). NH ($A \rightarrow X$) emission is observed under similar conditions.[7] In both observations the fuel consists of monomethyl hydrazine ($CH_3NH–NH_2$, MMH) oxidized by N_2O_4. The combustion products, which are thought to contain HCN and some unburnt MMH, react with the atmosphere near 300 km. The atmosphere consists of approximately 95% ground-state O(^3P) atoms and 2% N_2 at this orbital altitude. Understanding the nature and causes of these optical emissions is important for space-borne platforms, such as astronomical observatories.

Some studies of O-atom reactions at thermal energies have been reported. Becker and Bayes[8] observed intense emissions in atomic oxygen (AO)-hydrazine flames in the NO γ-bands ($A\ ^2\Sigma \rightarrow X\ ^2\Pi$), and weaker emissions in the OH($A\ ^2\Sigma \rightarrow X\ ^2\Pi$) and NH($A\ ^3\Pi \rightarrow X\ ^3\Sigma$) bands. Dimpfl *et al.*[9] observed infrared radiation from vibrationally-excited products of the reaction of O(^3P) with N_2H_4, $CH_3NH–NH_2$, and $CH_3NH–NHCH_3$ in a flow-tube study at room temperature. Rate constants for AO reactions measured at room temperature were found to be $(0.99\pm0.12)\times10^{-11}$, $(1.6\pm0.34)\times10^{-11}$, and $(2.3\pm0.34)\times10^{-11}$ cm^3 molecule^{-1} s^{-1} for N_2H_4, $CH_3NH–NH_2$, and $(CH_3)_2N–NH_2$, respectively.[10]

II. EXPERIMENTAL METHODS

The AO source, target region, and spectrometer system used in these measurements were the same as those used previously in single-collision, beam–beam studies of the gaseous targets H_2O, CO_2,[1] and HCN.[3] Briefly, the collision measurements are carried out in a uniform, high-intensity (6 T) solenoidal magnetic field (see Fig. 1 of Ref. 11). Magnetically-confined electrons of 8.0 eV energy resonantly attach to a beam of NO to form N+O$^-$(^2P). The magnetically-confined O$^-$ ions are accelerated to the desired final energy, and are separated from the electrons by a trochoidal deflector. The electrons are photodetached from the O$^-$ ions using all visible lines from a 20 W argon-ion laser in a multiple-pass geometry. The detachment fraction is 8%–15%, depending upon the velocity of the O$^-$ ions through the detachment region. The resulting O atoms are left exclusively in the ground ^3P state.[12] The O and (undetached) O$^-$ beams are then directed towards the hydrazine target. The O$^-$ ions and any photodetached electrons are reflected prior to reaching the hydrazine beam by a negative bias on the photon-collection mirror upstream of the target.

The neutral beam of each of the hydrazines is formed by effusion through a 1.0 mm diam hypodermic needle. The

 0021-9606/94/101(10)/8297/5/$6.00

target region was differentially pumped with a cryopump to maintain a pressure difference of 1.3×10^{-4} Pa (source) and 2.7×10^{-6} Pa (target) during operation. Base pressures were 1×10^{-6} Pa and 7×10^{-8} Pa at the source and target, respectively. Optical emissions from the collision region are collected with a spherical mirror and focused onto the entrance plane of a double-grating monochromator. Separate spectra of the emissions and backgrounds are recorded via multichannel scaling. The spectral resolution is 4.0 nm [full-width at half-maximum (FWHM)]. The principal sources of backgrounds are O^- collisions with surfaces, and in the wavelength range 450–550 nm scattered light from the argon-ion laser and the directly-heated electron emitter filament.

The hydrazines were obtained commercially[13] and had a stated purity of greater than 98%. Each of the hydrazines was contained in a Pyrex vial, and was subjected to ten freeze–thaw cycles with liquid nitrogen to remove dissolved gases. All valves and transfer lines were stainless steel.

III. EMISSION SPECTRA AND IDENTIFICATION

The relation between laboratory (LAB) and center-of-mass (CM) energies is given by the standard expression,[14]

$$E_{\mathrm{CM}}=\frac{m_1m_2}{m_1+m_2}\left[\frac{E_1}{m_1}+\frac{E_2}{m_2}-2\left(\frac{E_1E_2}{m_1m_2}\right)^{1/2}\cos\theta\right], \quad (1)$$

where m_i and E_i are masses and laboratory energies (subscripts 1,2 refer to O and the hydrazine or substituted hydrazine target, respectively). The energy of the hydrazines molecules in the beam is thermal (E_2=0.04 eV), and the angle θ between the AO and molecular beams is centered at 90° for crossed-beams collisions, with a total angular width $2\Delta\theta$ estimated to be at most 20°. Contribution from the second term in Eq. (1) (order of 0.01 eV CM energy) is neglected, as is the effect (third term, order of 0.01 eV CM energy) of the $2\Delta\theta$ width. The second and third terms are also of opposite sign and cancel at the 10^{-3} eV level. In this case Eq. (1) reduces to

$$E_{\mathrm{CM}}=0.667E_1 \quad [N_2H_4], \quad (2a)$$

$$E_{\mathrm{CM}}=0.742E_1 \quad [(CH_3)NH\text{–}NH_2], \quad (2b)$$

$$E_{\mathrm{CM}}=0.790E_1 \quad [(CH_3)_2N\text{–}NH_2]. \quad (2c)$$

Equation (1) is based only upon the laboratory energies of the incident particles, and gives no information on the energy sharing between the outgoing particles in the given reaction channel.

Shown in Fig. 1 are spectra resulting from the collisions of fast $O(^3P)$ atoms and each of the hydrazines. The laboratory O-atom energy was fixed at 20.0 eV in each case, corresponding to CM energies of 13.3 eV (hydrazine), 14.8 eV [monomethylhydrazine (MMH)], and 15.8 eV [1,1-dimethylhydrazine (1,1-DMH)]. All three hydrazines emit in the NH $A\ ^3\Pi\rightarrow X\ ^3\Sigma^-$ electronic system. In addition, we observe for 1,1-DMH emission in the CH $A\ ^2\Delta\rightarrow X\ ^2\Pi_r$ and CN $B\ ^2\Sigma^+\rightarrow X\ ^2\Sigma^+$ systems. No emissions were detected in the hydrazines for the range 550–850 nm.

Calculations of the relative emission intensity for each molecule were carried out in terms of the known energy

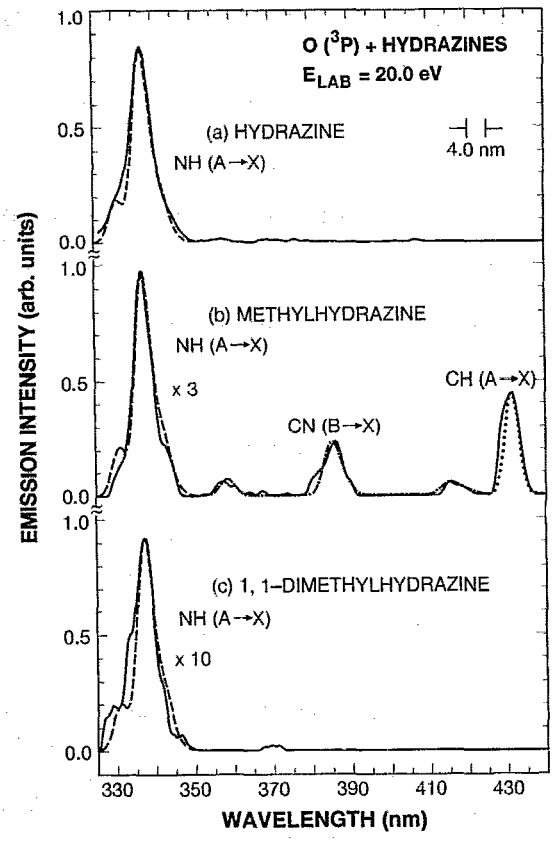

FIG. 1. Measured and simulated spectra of the CH $A\rightarrow X$, CN $B\rightarrow X$, and NH $A\rightarrow X$ emission systems in the wavelength range 325–440 nm, at a LAB energy of 20 eV for (a) hydrazine; (b) MMH; and (c) 1,1-DMH. Emission intensities may be intercompared within a spectrum and between spectra. The spectral resolution is 4.0 nm (FWHM). Simulations of each feature are indicated by the lines ---, -·-, and ···.

levels of the ground and excited electronic states of CH, CN, and NH, Franck–Condon factors for the vibrational bands, and the spectrometer slit function. The goal of this effort was to identify the emitting species and to characterize the lineshape of the emission in terms of a rotational (r) and vibrational (v) "temperature." These r,v temperatures may not be thermal, but serve as a means of characterizing the energy partition within the 4.0 nm spectral resolution.

The starting equation for the simulation is the emission intensity $I_{v'J',v''J''}$ between upper vibration-rotation levels $v'J'$ and lower levels $v''J''$. This intensity can be written in standard form as (see Ref. 15, p. 20),

$$I_{v'J',v''J''}=\left(\frac{64\pi^4c}{3}\left|R_e\right|^2\right)\frac{N_{v'J'}(T_v,T_r)}{2J'+1}\times\sigma^4_{v'J',v''J''}q(v',v'')S_{J'}. \quad (3)$$

Here, $N_{v'J'}(T_v,T_r)$ is the upper-state population corresponding to separate vibrational and rotational temperatures, $\sigma_{v'J',v''J''}$ the wave number of the transition, $q(v',v'')$ the Franck–Condon factor, $S_{J'}$ the rotational line strength, and

TABLE I. Summary of rotational and vibrational temperatures for the emitting species. All temperatures are in 10^3 K.

Species	NH		CN		CH	
	T_v	T_r	T_v	T_r	T_v	T_r
N_2H_4	10±1	4±0.5	a		a	
$CH_3NH–NH_2$	10±1	4±0.5	5±0.5	b	10±1	5±1
$(CH_3)_2N–NH_2$	10±1	4±0.5	a		a	

[a]No emission observed.
[b]Simulation insensitive to rotational temperature due to small rotational spacing relative to the spectral bandwidth.

$|R_e|^2$ the square of the electronic contribution to the transition moment, taken to be independent of internuclear separation for the present studies. The upper-state population $N_{v'J'}(T_v, T_r)$ was calculated from the Maxwell–Boltzmann distribution

$$N_{v'J'}(T_v, T_r) = N_{\text{tot}} \frac{e^{-\Delta E_v/kT_v}}{Q_v(T_v)} \times (2J'+1) \frac{e^{-B_v J'(J'+1)/kT_r}}{Q_R(T_r)}, \quad (4)$$

where ΔE is the vibrational energy, B_v the rotational constant in the emitting state, and $Q_v(T_v)$, $Q_r(T_r)$ the vibrational and rotational partition functions, respectively. Note that the vibration and rotation temperatures are not necessarily the same. The zero of energy is taken as that of the $v'=0$, $J'=0$ level of the emitting state. The final intensity was the sum over all upper levels significantly populated at each T_v and T_R with Franck–Condon factors greater than 0.04. This summed intensity was then convolved with a Gaussian spectrometer slit function of width 4.0 nm (FWHM) to obtain the final simulation.[1]

Energy-level data and rotational constants for CH, CN, and NH were taken from Huber and Herzberg.[16] Franck–Condon factors for CH $A \rightarrow X$ were taken from Liszt and Smith;[17] for CN $B \rightarrow X$ from Lavendy *et al.*;[18] and for NH $A \rightarrow X$ from Smith and Liszt.[19] The rotational line strengths $S_{J'}$ for the CN $B \rightarrow X$ transition were taken from Schadee (see Ref. 20, Table III); for the NH $A \rightarrow X$ transition from Schadee (see Ref. 20, Table V); and for the CH $A \rightarrow X$ transition from Kovacs.[21]

IV. DISCUSSION

Results of the spectral fitting are shown in Fig. 1, and the vibrational and rotational temperatures, as obtained from a best (visual) fit to the data, are summarized in Table I. Because of the small ratio between the rotational B-values ($\sim$15 cm^{-1}) and the spectral bandwidth ($\sim$250 cm^{-1} at 400 nm), the spectral fitting is not sensitive to T_r.

Because of the small emission cross sections in the hydrazines [approximately 0.01 of the emission cross sections encountered in HCN (Ref. 3)], we were unable in this case to explore the interesting energy dependence of the emissions below 20 eV, especially to establish energy thresholds and hence reaction channels leading to excitation of the band systems. Despite this fact, one can speculate on the possible reaction paths leading to the observed products. A listing of some of the most probable paths to produce CH, CN, and NH is presented in Table II. Center-of-mass (CM) threshold energies for production of the species in their ground states is given in the third column. Threshold energies for production of CH (A), CN (B), and NH (A) are obtained by adding electronic excitation energies (taken at their approximate onsets, see Fig. 1) of 2.83, 3.17, and 3.59 eV, respectively. The enthalpies of formation used to calculate the threshold are listed in Table III.

In discussing the data several points should be kept in mind. First, the results herein are under single-collision conditions, so that multiple-collision (secondary) reaction products are absent. This is relevant when comparing the present work with previous studies in (higher pressure, multiple-collision) flow tubes. Second, only photon-emitting species

TABLE II. Threshold energies in the center-of-mass (CM) and laboratory (LAB) frames for reactions of $O(^3P)$ and the hydrazines. All species are taken in their ground rotational, vibrational, and electronic states. Emitting species are indicated in bold type.

Reaction number	Reaction	Threshold energy (eV) CM	LAB
1	$O+N_2H_4 \rightarrow \mathbf{2NH}+H_2O$	1.73	2.60
2	$O+N_2H_4 \rightarrow \mathbf{NH}+OH+NH_2$	2.69	4.04
3	$O+CH_3NH–NH_2 \rightarrow \mathbf{NH}+CH_3NH(OH)$	−0.18	−0.25
4	$O+CH_3NH–NH_2 \rightarrow \mathbf{NH}+CH_3N+H_2O$	−0.78	−1.05
5	$O+(CH_3)_2N–NH_2 \rightarrow \mathbf{NH}+CH_3NH+CH_3O$	2.51	3.17
6	$O+(CH_3)_2N–NH_2 \rightarrow \mathbf{CH}+\mathbf{NH}+H_2O+CH_3NH$	6.02	7.62
7	$O+(CH_3)_2N–NH_2 \rightarrow \mathbf{NH}+CH_3NH(CH_3O)$	0.05	0.06
8	$O+(CH_3)_2N–NH_2 \rightarrow \mathbf{CN}+CH_3NH_2+H_2O+H$	0.57	0.73

TABLE III. Auxiliary thermodynamic data. All heats of formation are taken from the compilation by Stein (Ref. 22). Conversion to the eV scale is 23.06 kcal/mol=1 eV.

Species	$\Delta H_f(g,298\ \mathrm{K})$, kcal/mol
O	+59.6
OH	+9.3
CH	+142.4
NH	+90.0
H_2O	−57.8
N_2H_4	+22.8
CH_3–NH–NH_2	+22.6
$(CH_3)_2$N–NH_2	+20.0
NH_2	+45.1
CH_3NH	+43.6
CH_3NH_2	−5.5
CH_2=NH	+3.7
CH_3O	+3.7
CH_3O–NH_2	−6
$CH_3NH(OH)$	−12

radiating in the range 300–850 nm are detectable. "Dark" molecules which either radiate outside this range, or which do not radiate at all, are not observed.

In considering the dynamics of the reactions we note that the NH ($A\rightarrow X$) emission is common to the three molecules. Dimpfl *et al.*[9] studied the thermal reactions of $O(^3P)$ with N_2H_4, CH_3NH–NH_2, and CH_3NH–$NHCH_3$ in a flow tube and observed infrared emission from OH, H_2O, CO, CO_2, HNO, and H_2CO. The most relevant observation is that $O(^3P)+N_2H_4$ leads to emission from $OH(v)$ and $H_2O(v)$, where v indicates vibrational excitation. For these thermal-energy reactions it is possible that single-collision processes can give rise to the observed products,

$$O+N_2H_4\rightarrow OH(v)+N_2H_3, \tag{5a}$$

and

$$O+N_2H_4\rightarrow H_2O(v)+N_2H_2^*, \tag{5b}$$

followed by

$$N_2H_2^*\rightarrow 2NH. \tag{5c}$$

Likewise for the cases of CH_3NH–NH_2, and CH_3NH–$NHCH_3$ the generation of $OH(v)$ and $H_2O(v)$ may proceed under single-collision conditions, while the generation of CO or CO_2 must involve multiple collisions.

The observed products NH, CN, and CH in the case of methylhydrazine are present in the ratio 1.0, 0.23, and 0.45, respectively. The most likely path for NH is through a complex rearrangement

$$O+CH_3NH-NH_2\rightarrow NH+CH_3NH-OH, \tag{6}$$

a process which is endothermic by ~0.2 eV. Thus the added CM collision energy is essential to the formation of NH in the $A\ ^3\Pi$ state. The only optically-active product observed in the case of 1,1-DMH is NH, which suggests that the primary reaction is an impulsive collision

$$O+(CH_3)_2N-NH_2\rightarrow NH+CH_3NH-CH_3O, \tag{7}$$

which is endothermic by ~0.05 eV.

Experimentally, the intensity of NH emission in the series N_2H_4:MMH:1,1-DMH is observed as 1.0:0.38:0.11 (Fig. 1). This is counter to the trend of the thermal-energy rate coefficients (1.0:1.6:2.3),[10] and to the decreasing endothermicity between Reactions (6) and (7). The different trends are almost certainly due to the fact that the reaction-rate coefficients were measured at thermal $O(^3P)$ energies (E_{CM}~0.04 eV), while present data are at an energy two orders-of-magnitude higher [Reactions (2)] where new reaction channels and intermediates come into play. Also, present data involve only single AO-molecule collisions, whereas the rate constants are measured under multiple collisions. Finally, with increasing complexity of the hydrazine target, the intermediate state may rearrange more easily into fragments other than NH. And hence the observed trend in emission intensity corresponds to a partition of the excess energy into more open exit channels.

Finally, it is interesting to speculate as to why the CH $B\rightarrow X$ emission is absent in Fig. 1(b). If the B state is populated equally, it should be present at about half the intensity of the CH $A\rightarrow X$ emission.[16] We conclude either that (a) there is a potential barrier for decay of the O·MMH complex to CH (B), or that (b) some other competing channel is stealing most of the outgoing flux.

ACKNOWLEDGMENTS

This work was carried out at the Jet Propulsion Laboratory, California Institute of Technology, and the Air Force Phillips Laboratory. It was supported by the AFOSR and the Phillips Laboratory through agreement with the National Aeronautics and Space Administration.

[1] O. J. Orient, A. Chutjian, and E. Murad, Phys. Rev. Lett. **65**, 2359 (1990).
[2] O. J. Orient, K. E. Martus, A. Chutjian, and E. Murad, J. Chem. Phys. **97**, 4111 (1992).
[3] O. J. Orient, A. Chutjian, K. E. Martus, and E. Murad, Phys. Rev. A **48**, 427 (1993).
[4] R. D. Levine and R. B. Bernstein, *Molecular Reaction Dynamics* (Oxford University, United Kingdom, 1974); *Molecular Reaction Dynamics and Chemical Reactivity* (Oxford University, United Kingdom, 1987).
[5] I. W. M. Smith, *Kinetics and Dynamics of Elementary Gas Reactions* (Butterworth, London, 1980), pp. 318–320.
[6] R. A. Viereck, L. S. Bernstein, S. B. Mende, E. Murad, G. R. Swenson, and C. B. Pike, J. Space. Rockets **30**, 724 (1993).
[7] A. L. Broadfoot, E. Anderson, P. Sherard, J. W. Chamberlain, D. J. Knecht, R. A. Viereck, C. P. Pike, E. Murad, J. B. Elgin, L. S. Bernstein, I. L. Kofsky, D. L. A. Rall, and J. Culbertson, J. Geophys. Res. A **97**, 19 501 (1992).
[8] K. H. Becker and K. D. Bayes, J. Phys. Chem. **71**, 371 (1967).
[9] W. Dimpfl, L. S. Bernstein, S. M. Adler-Golden, J. W. Cox, K. W. Cunningham, and A. T. Pritt (in preparation).
[10] V. I. Lang, J. Phys. Chem. **96**, 3047 (1992).
[11] O. J. Orient, K. E. Martus, A. Chutjian, and E. Murad, Phys. Rev. A **45**, 2998 (1992).
[12] L. M. Branscomb, S. J. Smith, and G. Tisone, J. Chem. Phys. **43**, 2906 (1965).
[13] Aldrich Chemical Co., Milwaukee, Wisconsin 53233.
[14] K. T. Dolder and B. Peart, Rep. Prog. Phys. **39**, 693 (1976).
[15] G. Herzberg, *Molecular Spectra and Molecular Structure I. Spectra of Diatomic Molecules* (Van Nostrand, New York, 1950), p. 127.

[16] K. P. Huber and G. Herzberg, *Molecular Spectra and Molecular Structure IV. Constants of Diatomic Molecules* (Van Nostrand Reinhold, New York, 1979), p. 154 (CN).
[17] H. S. Liszt and W. H. Smith, J. Quant. Spectrosc. Radiat. Transfer **12**, 947 (1972).
[18] H. Lavendy, G. Gandara, and J. M. Robbe, J. Mol. Spectrosc. **106**, 395 (1984).
[19] W. H. Smith and H. S. Liszt, J. Quant. Spectrosc. Radiat. Transfer **11**, 45 (1971).
[20] A. Schadee, Bull. Astron. Inst. Netherlands **17**, 311 (1964).
[21] I. Kovacs, *Rotational Structure in the Spectra of Diatomic Molecules* (American Elsevier, New York, 1969), Chap. 3.
[22] S. E. Stein, NIST Standard Reference Database No. 25, NIST Structures and Properties (available on disk from NIST, Gaithersburg, MD 20899).